V European Conference on Computational Fluid Dynamics
ECCOMAS CFD 2010
J. C. F. Pereira and A. Sequeira (Eds)
Lisbon, Portugal,14-17 June 2010

CALIBRATING REDUCED DIMENSION MODELS FOR 3D PATIENT SPECIFIC FLUID-STRUCTURE INTERACTION SIMULATIONS

Mahmoud Ismail*, Michael W. Gee*, Andrew Comerford*, Wolfgang A. Wall*

*Institute for Computational Mechanics
Technische Universität München, Boltzmannstr. 15, 85747 Garching b. München, Germany
e-mail: {ismail, gee, comerford, wall}@lnm.mw.tum.de

Key words: Hemodynamics, Reduced-Dimension Models, Inverse Analysis, Computational Bioflow, Fluid Dynamics, Fluid-Structure-Interaction

Abstract. *Simulating patient specific biofluid networks, such as blood flow in arteries, requires a complete modeling of the system. This is essential to capture physiological pressure values within such systems. However, the three-dimensional discretization of these complete networks is neither necessary nor regularly achievable with the current computing power. The latter is especially true when fluid-structure interaction (FSI) effects have to be included. Therefore, three-dimensional FSI models are trimmed at the boundary of a region of interest and coupled to zero-dimensional, one-dimensional, and lumped models, which in turn are capable of mimicking the physical behavior of the smaller parts of the network. Unfortunately, calibrating these models to obtain desired physiological pressures within three-dimensional FSI geometries has received little attention. For this reason, this work covers the implementation of reduced-dimension models, the coupling between reduced and three-dimensional FSI models and the calibration of the reduced models using inverse analysis methods. All of the mentioned tasks were applied to three-dimensional patient specific geometries of vasculature.*

1 INTRODUCTION

Computational modeling, such as finite-element simulation (FE), has proven to be very a useful and important tool for a better understanding of the biomechanical behavior of the human vasculature. This is particularly significant for diseased arteries such as when aneurysms occur [3, 4]. In this case, geometries such as *abdominal aortic aneurysms (AAA)* require special treatment of the outflow boundary conditions to reproduce the physiological blood pressure within the biogeometry. Such blood pressure can be produced by the impedance outlet boundary conditions [3]. Among impedance models, *windkessel* is one of the most popular. Unfortunately, experimental calibration of such models is highly dependent on the state and the position in which the patient was tested [5]. This also means that wrong estimation of *windkessel* parameters might generate nonphysiological pressure values. Spilker and Taylor [9] have successfully tuned *windkessel* parameters by solving a nonlinear minimization problem using Broyden's method, which computes the *Jacobian* of the minimization problem from previous *Jacobian* update. In other words, Broyden's method requires only the initial *Jacobian* to be evaluated. Since evaluation of the *Jacobian* by finite difference is too expensive in 3D patient specific geometries, Spilker and Taylor [9] suggested using reduced-dimensional models (such as one-dimensional FSI models [8]) to compute the initial *Jacobian*. Such a methodology is likely to be challenging especially in geometries such as aneurysms. Thus we propose to use an adjoint method, which can compute the *Jacobian* without finite differences and independent of the previous minimization step [2].

2 METHODOLOGY

2.1 3D Geometry Reconstruction

The geometry in Fig 1 was extracted from a patients CT scan. Both lumen and intraluminal thrombus (ILT) were segmented in Mimics and 3-matics (Materialise). The arterial wall was generated using a custom extrusion algorithm.

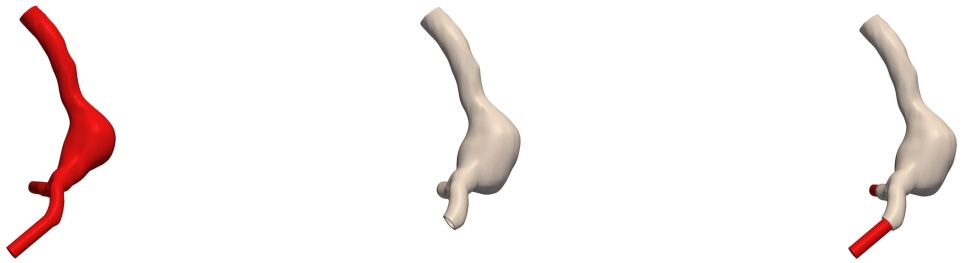

(a) (b) (c)

Figure 1: Segmented *abdominal aortic aneurysm* showing the different domains inside. (a) AAA fluid domain. (b) AAA structural domain including intraluminal thrombus and artery wall. (c) AAA fluid-structural domain and extruded common iliacs

2.2 Windkessel Model

A three-element *windkessel* model shown in Fig 2 is represented by the following differential equation:

$$\mathbf{N} : p + CR_2\frac{dp}{dt} - (R_2 + R_1)\, q - CR_1R_2\frac{dq}{dt} = 0 \tag{1}$$

where p_C^- and p_{out} are set to zero [5], p_{in} and q_{in} are renamed to p and q, respectively.

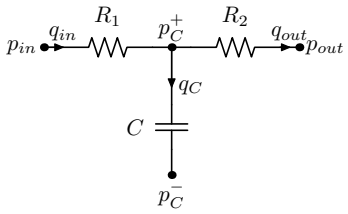

Figure 2: Circuit representation of a three-element windkessel model

Making use of the periodicity of the cardiac cycle, eq (1) is solved, using impedance methods, with the help of periodic Fourier transformation [5, 6] and implemented in our *in house* multi-physics research code BACI [1, 10].

2.3 Adjoint Method

Consider the optimization problem:

$$\min \mathbf{L}\,(u, \phi) \tag{2}$$
$$\text{subject to } \mathbf{N}\,(u, \phi) = 0 \tag{3}$$

where $\mathbf{L}$ is the objective functions, $\mathbf{N}$ the governing equations, u the state variables, and ϕ the design variables. To optimize the cost function $\mathbf{L}$, a *Jacobian* $\mathbf{J}$ must be computed.

$$\mathbf{J} = \frac{d\mathbf{L}}{d\phi} = \frac{\partial \mathbf{L}}{\partial u}\frac{du}{d\phi} + \frac{\partial \mathbf{L}}{\partial \phi} \tag{4}$$

Looking at eq (4), it is noticed that $\frac{du}{d\phi}$ is the only unknown term, which is evaluated from the governing equations ($\mathbf{N}$) as:

$$\frac{d\mathbf{N}}{d\phi} = \frac{\partial \mathbf{N}}{\partial u}\frac{du}{d\phi} + \frac{\partial \mathbf{N}}{\partial \phi} = 0 \tag{5}$$

thus

$$\frac{du}{d\phi} = \left(\frac{\partial \mathbf{N}}{\partial u}\right)^{-1}\left(-\frac{\partial \mathbf{N}}{\partial \phi}\right) \tag{6}$$

finally

$$\mathbf{J} = -\left(\frac{\partial \mathbf{L}}{\partial u}\right)\left(\frac{\partial \mathbf{N}}{\partial u}\right)^{-1}\left(\frac{\partial \mathbf{N}}{\partial \phi}\right) + \frac{\partial \mathbf{L}}{\partial \phi} \tag{7}$$

Then, design variables are updated by directly solving

$$\phi^n - \phi^{n+1} = \mathbf{J}^{-1} \cdot \mathbf{L}\left(u^n, \phi^n\right) \tag{8}$$

3 Results

The theories in sections 2.2 and 2.3 are tested on a patient specific aorta extracted from a patient with an Abdominal Aortic Aneurysm (AAA). A volumetric flow rate was prescribed at the inlet, and two three-element windkessel boundary conditions were prescribed at the corresponding common iliac outlets. Windkessel parameters were calibrated using the optimization method in section 2.3 with an objective function:

$$\mathbf{L}\left(u, \begin{bmatrix} R \\ C \end{bmatrix}\right) = \begin{bmatrix} \left| \begin{array}{c} P_{maximum} - P_{systolic} \\ P_{minimum} - P_{diastolic} \end{array} \right| \end{bmatrix} = \begin{bmatrix} 0 \\ 0 \end{bmatrix} \tag{9}$$

$\mathrm{P}_{systolic}$ and $\mathrm{P}_{diastolic}$ were considered 120 mmHg and 80 mmHg, respectively. Total resistance ($R = R_1 + R_2$) and capacitance (C) were chosen as design variables.

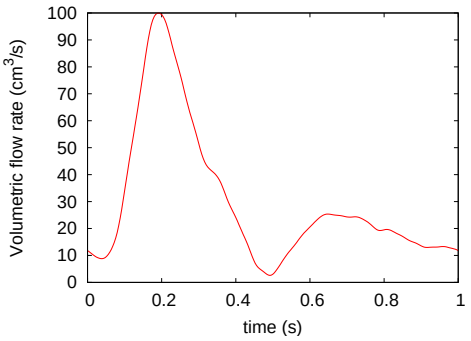

Figure 3: Volumetric flow rate prescribed at the aortic inlet

The wall thickness of the AAA was taken as 1.2mm and the wall material was assumed to be isotropic, incompressible, and hyperelastic with $\alpha = 0.174MPa$ and $\beta = 1.881MPa$ [7]. The intraluminal thrombus was assumed to be compressible Neo-Hookean material with Youngs modulus $E = 0.1044MPa$ and Poisson's ratio $\nu = 0.45$. The blood was assumed to be Newtonian fluid with density $\rho = 1000Kg/m^3$ and dynamic viscosity $\mu = 4mPas.s$.

Both outlets were initially calibrated to the windkessel parameters shown in Table 1. The inlet boundary condition was prescribed by the volumetric flow rate profile in Fig 3. The final results are shown in Fig 4, where outlet pressure curves at different optimization steps show that desired pressure peaks were obtained after the second optimization step. This also could be noticed from the second norm of the objective function which is presented in Fig 5.

Table 1: Windkessel element parameters before and after the optimization

Left common iliac			Right common iliac		
Parameters	Initial	Final	Parameters	Initial	Final
$R_1\,[Pa \cdot s \cdot mm^{-3}]$	0.07	0.0787803	$R_1\,[Pa \cdot s \cdot mm^{-3}]$	0.07	0.078904
$R_2\,[Pa \cdot s \cdot mm^{-3}]$	0.70	0.7878030	$R_2\,[Pa \cdot s \cdot mm^{-3}]$	0.70	0.789040
$C\ [Pa^{-1} \cdot mm^3]$	1.50	1.3780100	$C\ [Pa^{-1} \cdot mm^3]$	1.50	1.376280

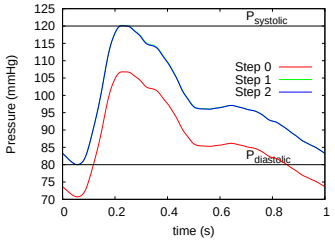

(a) Pressure during different minimization steps in the left iliac

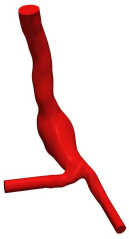

(b)

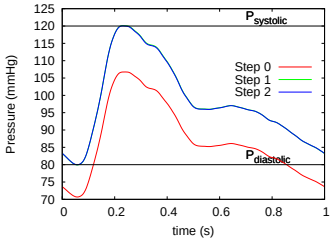

(c) Pressure during different optimization steps in the right iliac

Figure 4: Optimization results at the common iliac outlets

4 CONCLUSIONS

Special treatment of the outflow boundary conditions of patient specific vasculature problems using reduced-dimensional hemodynamic models is not enough. Calibrating such models is essential to reproduce the correct physiological blood pressure. Further investigation of different objective functions is required for better representation of the physiological information.

5 Acknowledgments

The authors gratefully acknowledge support through the International Graduate School of Science and Engineering (IGSSE) of the Technische Universität München, Germany,

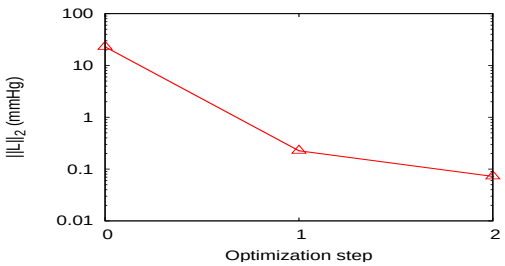

Figure 5: The L_2 norm of the objective function at different optimization steps

under project 2–11 and 3–7.

References

[1] A. Comerford, Ch. Förster, and W.A. Wall. Structured tree impedance outflow boundary conditions for 3d lung simulations. *Journal of Biomechanical Engineering*, accepted, 2010.

[2] Austen C. Duffy. An introduction to gradient computation by the discrete adjoint method. Technical report, Florida State University, Summer 2009.

[3] J.D. Humphrey and C.A. Taylor. Intracranial and abdominal aortic aneurysms: Similarities, differences, and need for a new class of computational models. *Annual Review of Biomedical Engineering*, 10:221–46, 2008.

[4] A. Maier, M.W. Gee, C. Reeps, J. Pongratz, H.-H. Eckstein, and W.A. Wall. A comparison of diameter, wall stress and rupture potential index for abdominal aortic aneurysm rupture risk prediction. *Annals of Biomedical Engineering*, Submitted, 2010.

[5] M. S. Olufsen, A. Nadim, and L. A. Lipsitz. Dynamics of cerebral blood flow regulation explained using a lumped parameter model. *American Journal of Physiology Regulatory, Integrative and Comparative Physiology*, 282:611–622, 2002.

[6] M.S. Olufsen, C.S. Peskin, W. Y. Kim, E. M. Pedersen, A. Nadim, and J. Larsen. Numerical simulation and experimental validation of blood flow in arteries with structured-tree outow conditions. *Annals of Biomedical Engineering*, 28:12811299, 2000.

[7] M. L. Raghavan and D. A. Vorp. Toward a biomechanical tool to evaluate rupture potential of abdominal aortic aneurysm: identification of a finite strain constitutive model and evaluation of its applicability. *Journal of Biomechanics*, 33(4):475–482, April 2000.

[8] S. J. Sherwin, L. Formaggia, J. Peiro, and V. Franke. Computational modelling of 1d blood flow with variable mechanical properties and its application to the simulation of wave propagation in human arterial system. *International Journal for Numerical Methods in Fluids*, 43:673–700, 2003.

[9] R. L. Spilker and C. A. Taylor. Tuning a multiscale model of abdominal aortic hemodynamics to incorporate patient-specific features of flow and pressure waveforms. In *ASME Summer Bioengineering Conference*, 2009.

[10] W. A. Wall and M. W. Gee. Baci: A parallel multiphysics finite element environment. Technical report, Institute for Computational Mechanics, Technische Universität München, 2010.